MOLECULAR AND CELLULAR BIOLOGY, Jan. 2003, p. 425–436 Vol. 23, No. 2
0270-7306/03/$08.00+0 DOI: 10.1128/MCB.23.2.425–436.2003

p38 Mitogen-Activated Protein Kinase-Dependent and -Independent Signaling of mRNA Stability of AU-Rich Element-Containing Transcripts

Mathias A. E. Frevel,[1] Tala Bakheet,[2] Aristobolo M. Silva,[1] John G. Hissong,[1] Khalid S. A. Khabar,[1,2] and Bryan R. G. Williams[1]*

Department of Cancer Biology, Lerner Research Institute, Cleveland Clinic Foundation, Cleveland, Ohio 44195,[1] *and Department of Biostatistics, Epidemiology and Scientific Computing and Department of Biological and Medical Research, King Faisal Specialist Hospital and Research Center, Riyadh 11211, Saudi Arabia*[2]

Received 13 June 2002/Returned for modification 6 August 2002/Accepted 1 October 2002

Adenylate/uridylate-rich element (ARE)-mediated mRNA turnover is an important regulatory component of gene expression for innate and specific immunity, in the hematopoietic system, in cellular growth regulation, and for many other cellular processes. This diversity is reflected in the distribution of AREs in the human genome, which we have established as a database of more than 900 ARE-containing genes that may utilize AREs as a means of controlling cellular mRNA levels. The p38 mitogen-activated protein kinase (MAP kinase) pathway has been implicated in regulating the stability of nine ARE-containing transcripts. Here we explored the entire spectrum of ARE-containing genes for p38-dependent regulation of ARE-mediated mRNA turnover with a custom cDNA array containing probes for 950 ARE mRNAs. The human monocytic cell line THP-1 treated with lipopolysaccharide (LPS) was used as a reproducible cellular model system that allowed us to precisely control the conditions of mRNA induction and decay in the absence and presence of the p38 inhibitor SB203580. This approach allowed us to establish an LPS-induced ARE mRNA expression profile in human monocytes and determine the half-lives of 470 AU-rich mRNAs. Most importantly, we identified 42 AU-rich genes, previously unrecognized, that show p38-dependent mRNA stabilization. In addition to a number of cytokines, several interesting novel AU-rich transcripts likely to play a role in macrophage activation by LPS exhibited p38-dependent transcript stabilization, including macrophage-specific colony-stimulating factor 1, carbonic anhydrase 2, Bcl2, Bcl2-like 2, and nuclear factor erythroid 2-like 2. Finally, the identification of the p38-dependent upstream activator MAP kinase kinase 6 as a member of this group identifies a positive feedback loop regulating macrophage signaling via p38 MAP kinase-dependent transcript stabilization.

The regulation of mRNA stability is an important factor in modulating gene expression, in particular for transiently expressed genes that require tightly controlled mRNA levels. For different cytokines, growth factors, and proto-oncogenes with short mRNA half-lives, modulating the decay rate involves adenylate/uridylate (AU)-rich elements (AREs), often consisting of one to several copies of the sequence AUUUA located in the 3′ untranslated region (12). With a bioinformatics approach, we previously identified several hundred ARE-containing genes that were compiled in the ARE mRNA database (ARED) (2). These genes encode a wide variety of proteins, implicating ARE-mediated mRNA decay in a broader spectrum of cellular processes than was previously recognized.

The molecular mechanisms by which AREs are used to fine-tune mRNA turnover are thought to involve specific RNA-binding proteins (33, 34). *trans*-Acting factors from different protein families that bind AREs and influence mRNA degradation have been identified. The Hu family proteins HuR and HuB have been shown to bind many different AU-rich messages and stabilize these in several different cell systems (22, 24, 25, 30, 41, 42, 44, 46, 55, 59). AUF1/heterogeneous nuclear ribonucleoprotein D binds to and destabilizes ARE mRNAs such as c-*myc*, granulocyte-macrophage colony-stimulating factor and others (5, 18, 43, 70). Recently, AUF1 was implicated in apoptosis as a binding factor of the Bcl2 ARE and in tumorigenesis, causing tumor development when overexpressed in mice (26, 37). Tristetraprolin, a protein from the CCCH tandem zinc finger family, appears to regulate mRNA stability of tumor necrosis factor alpha, granulocyte-macrophage colony-stimulating factor, and interleukin-3 (7, 8, 35, 62).

The stabilizing and destabilizing activities of ARE-binding factors can in turn be regulated via a network of signal transduction, giving cells the ability to respond to extra- and intracellular signals by fine-tuning decay rates of mRNAs critical to processes such as cell growth, differentiation, and immune response. The p38 mitogen-activated protein kinase (MAP kinase) pathway has been implicated in the regulation of the mRNA half-lives of a number of AU-rich genes, including cyclooxygenase 2 (*COX2*), tumor necrosis factor alpha, interleukin-3, interleukin-6, interleukin-8, macrophage-inhibitory protein 1α (MIP1α), granulocyte macrophage-colony stimulating factor, vascular endothelial growth factor, and urokinase-type plasminogen activator (4, 28, 47, 48, 54, 63, 67, 70).

COX2 mRNA levels greatly increase in monocytes upon bacterial lipopolysaccharide (LPS) treatment. This induction is due to transcriptional activation and message stabilization. Inhibition of p38 with the chemical inhibitor SB203580 (SB) or

* Corresponding author. Mailing address: 9500 Euclid Ave., Cancer Biology Department, NB40, Cleveland Clinic Foundation, Cleveland, OH 44195. Phone: (216) 445 9652. Fax: (216) 444 3164. E-mail: williab@ccf.org.

by expressing dominant negative MAP kinase-activated protein kinase 2, a kinase downstream of p38, abolishes stabilization and leads to rapid degradation of *COX2* mRNA (17, 39). How p38 signaling might link to ARE-binding proteins has recently been investigated for tristetraprolin. In vitro evidence shows that tristetraprolin can be directly phosphorylated by either p38 or MAP kinase-activated protein kinase 2, potentially modifying its destabilizing activity (6, 45). Alternatively, p38 may also phosphorylate ARE-stabilizing proteins that could compete with destabilizing proteins, as suggested for HuR and tristetraprolin in the case of regulating interleukin-3 decay (47).

To investigate the extent to which the p38 pathway is involved in regulating the mRNA decay of the entire spectrum of ARE-containing genes, we performed a large-scale analysis of AU-rich mRNA turnover with the AU array. This cDNA microarray with 950 ARE-containing and additional control genes was specifically constructed for this purpose. With this approach, we were able to determine the half-lives of 470 ARE mRNAs with and without p38 inhibition, allowing us to define 42 newly identified p38 MAP kinase target mRNAs.

MATERIALS AND METHODS

AU-rich gene array construction. The AU-rich gene array used in this study contained probes for 950 AU-rich genes from the ARED (2), 18 genes potentially involved in AU-directed mRNA decay, 50 housekeeping genes, and 4 positive control sequences of bacterial origin. Sequence-verified clones for these were obtained from the 40K human clone set (Research Genetics). cDNA inserts were PCR amplified according to Research Genetics instructions. PCR products were purified with size exclusion filter plates (Millipore, MANU030 PCR) and quality controlled by gel electrophoresis. DNA in 1.5× SSC (1× SSC is 0.15 M NaCl plus 0.015 M sodium citrate) was printed on poly-L-lysine home-coated slides with the SDDC-2 microarrayer (Virtek Vision Inc.). Every gene probe was printed in duplicate. After printing, slides were UV treated (120 mJ), incubated for 10 min in blocking solution (170 mM succinic anhydride, 70 mM sodium borate in 1-methyl-2-pyrrolidinone) and for 2 min in 95°C H_2O, and spun dry. These slides were used for hybridization from 2 days up to 2 months after printing with equally good results.

Cell culture, treatment, and sample preparation. THP-1 cells were cultured in RPMI (Invitrogen) with 10% fetal calf serum at 37°C with 5% CO_2 for 7 days prior to treatment. For treatments, cells were plated at 2.5×10^6 cells/ml in 25 ml of medium 1 h before adding drugs. LPS treatments (10 μg/ml, *Escherichia coli* serotype O111:B4; Sigma) were for 2 h. To measure RNA decay, actinomycin D (5 μg/ml, Sigma) alone or actinomycin D plus SB (1 μM, Calbiochem) was added to the LPS-treated cultures and harvested 30, 60, 90, 120, 180, and 240 min later for RNA and cell extract preparation. Cells were collected by sedimenting suspended cells and washing differentiating, adherent cells off the plate.

Total RNA was extracted with Trizol reagent (Invitrogen) according to the manufacturer's instructions. Whole-cell extracts were prepared after two washes with ice-cold phosphate-buffered saline with a lysis buffer containing 1% Triton X-100 as the detergent, supplemented with protease and phosphatase inhibitors (leupeptin, aprotinin, phenylmethylsulfonyl fluoride, sodium orthovanadate, and pepstatin). The LPS treatments were performed 13 times independently, giving rise to the gene induction-repression data in Table 1. The RNA decay time courses were performed three times on independently cultured THP-1 cells.

Western blotting. Whole-cell extracts (30 μg) were fractionated on sodium dodecyl sulfate (SDS)–10% polyacrylamide gels, transferred to a polyvinylidene difluoride membrane, and probed with anti-phospho-p38 and anti-p38 antibodies (New England Biolabs).

RNA labeling and array hybridization. For each array hybridization, RNAs from treated and untreated THP-1 cells were labeled with indocarbocyanine and indodicarbocyanine, respectively. The labeling reactions were standard cDNA syntheses incorporating labeled dUTP. The primer-annealing mixture contained 80 μg of total RNA, 2 μg of dT_{12-18} primer, 20 U of anti-RNase (Ambion), and 0.5 ng of each positive-control RNA in 33 μl. The four positive-control RNAs were obtained by in vitro transcription from poly(A) tail-modified bacterial gene constructs pGIBS-DAP, -PHE, -THR, and -TRP (American Type Culture Collection). The mixture was heated to 70°C for 10 min and cooled on ice.

Subsequent cDNA synthesis was at 42°C for 2 h in 50 μl with 400 U of Superscript II and 1× first-strand buffer (Invitrogen), 10 mM dithiothreitol, 0.5 mM each dATP, dCTP, and dGTP, 0.3 mM dTTP, and 3 nmol of carbocyanine-dUTP (New England Nuclear). The cDNA was purified with GFX columns following the manufacturer's instructions (Amersham Pharmacia Biotech), dried down, and resuspended in hybridization buffer containing 2× SSC, 0.1% SDS, 4 μg of $poly(dA)_{40-60}$, and 4 μg of yeast tRNA. The indocarbocyanine- and indodicarbocyanine-labeled cDNAs were pooled and hybridized to the array slide under a coverglass in a Corning Microarray Technology hybridization chamber at 65°C for 16 h. Subsequently, slides were washed successively for 5 min each with 2× SSC–0.1% SDS, 2× SSC, and 0.2× SSC, spun dry, and scanned on a GenePix 4000A scanner (Axon).

Array data acquisition and normalization. Raw fluorescence data were acquired with the GenePix software (Axon). Laser settings were chosen to avoid signal saturation and achieve an overall median indocarbocyanine/indodicarbocyanine ratio of 0.8 to 1.2. The raw data were imported into the GeneSpring software version 4.2 (Silicon Genetics) for further analysis. For each gene probe, the signal intensity ratio of the treated over the untreated sample was calculated with raw fluorescent intensities, with the local background subtracted. Fluorescent intensities of the untreated samples were set to a minimum value of 300 if below that. The ratios were then normalized based on the distribution of all values with locally weighted polynomial regression (LOESS). For the decay time courses, an additional normalization was necessary because the LOESS normalization localizes the overall mean of the ratios at 1, whereas the mean of ratios naturally decreases below 1 with successive decay of the treated sample. In order to recover reality, the ratios for each array were corrected so that the mean ratio of the four positive-control probes that had been spiked into every sample in a constant amount equaled 1. To be able to compare the RNA decay observed with and without the p38 inhibitor, the average ratios from the three sets of decay time courses were finally corrected for glyceraldehyde-3-phosphate dehydrogenase based on 14 glyceraldehyde-3-phosphate dehydrogenase probes on the array.

Half-life calculations. The natural logarithms of the average normalized ratios of treated over untreated samples (y) from three independent biological repeats with their respective standard deviations (σ) were plotted against the time (x). The samples taken after 2 h of LPS treatment represent the 0-min time point from which the RNA decay measurement started. In order to exclude genes expressed at levels that are below or close to the detection limit, genes with normalized raw fluorescent intensities in the treated sample of less than the overall average background (B) plus 1 standard deviation at the 0-min time point were excluded from analysis. Lines were fit to the log-transformed data with the least-squares regression. The $t_{1/2}$ was calculated as $(-\ln [2]/m)$, where m is the slope of the line fit to the data (3).

The linear regression fit was performed on from two to seven time points, and the χ^2 for each fit was calculated. The fit that gave the minimum χ^2 per degree of freedom was chosen for calculating the $t_{1/2}$. Differences in $t_{1/2}$ between decay with and without the p38 inhibitor were evaluated with a t-distributed statistic for distributions with unequal variances. The t statistic and the degree of freedom for the t statistic were processed to give a P value with SurfStat statistical tables online (K. Dear and R. Brennan, University of Newcastle [http://math.uc.edu/~brycw/classes/148/tables.htm]) (58). To avoid distorting the half-life calculation for rapidly decaying genes by using measurements taken at later time points, when the signal detected for this message has already reached background level, we made a second expression level cut and excluded measurements from time points when the normalized raw fluorescent intensity from the treated sample reached a level below $B + 2$ standard deviations.

Northern blotting. Total RNA was fractionated on 1% agarose gels containing 0.41 M formaldehyde, capillary transferred to positively charged nylon membrane with 10× SSC, and fixed by UV cross-linking. cDNA probes (25 ng) for *COX2*, interleukin-1β, interleukin-8, and glyceraldehyde-3-phosphate dehydrogenase were labeled with 50 μCi of [α-^{32}P]dCTP by random priming. Hybridization overnight was done at 65°C in 0.5 M sodium phosphate buffer, pH 7.2, with 7% SDS, 1 mM EDTA, and 10% dextran sulfate. Blots were washed twice in 2× SSC–0.1% SDS at 65°C and exposed to X-OMAT AR film (Kodak). Signals were quantified by densitometry with ImageQuant software (Molecular Dynamics).

RESULTS

ARE-containing gene transcription profile in THP-1 monocytes in response to LPS. Exposure of human monocytes, including THP-1 cells, to LPS is known to induce various genes,

TABLE 1. AU-rich mRNAs induced or repressed in THP-1 cells after 2 h of LPS treatment

Unigene symbol	Acc[a]	Fold change[b]	SE	Times >2-fold[c]	Unigene symbol	Acc	Fold change	SE	Times >2-fold
SCYA4 (MIP1β)	H62985	113.2	21.44	13/13	KCNA3	AI095381	2.5	0.50	6/11
IL1B	W47101	71.5	15.51	12/13	PARG1	AA629603	2.5	0.29	8/13
SCYA3L1	R47893	60.9	11.98	13/13	KIAA0254	N75979	2.5	0.49	7/13
IL8	IL8[d]	43.5	9.67	6/6	TFAP2C	AA399334	2.5	0.31	7/10
TNFAIP3	AA476272	42.1	5.53	13/13	CSF3	AI074784	2.5	0.49	5/13
NR4A3	H37761	37.2	10.71	13/13	ITGAV	AA029934	2.5	0.20	9/13
TNF	AA699697	31.3	6.63	13/13	PMAIP1	AA458838	2.4	0.64	7/13
GRO2	R50407	31.1	5.81	13/13	NR4A1	N94487	2.4	0.20	8/13
SCYA3 (MIP1α)	AA677522	28.9	4.06	12/12	RASGRP1	AA884877	2.4	0.39	6/11
GRO1	W42723	27.5	5.86	13/13	TLR3	R76099	2.3	0.10	10/13
PTGS2 (COX2)	R80217	27.3	6.50	13/13	KIAA0852	W80688	2.3	0.33	6/11
CPSF6	R18985	20.7	3.92	10/13	SNAI1	AA464983	2.3	0.27	7/13
GRO3	AA935273	19.7	4.10	13/13	DAF	R09561	2.3	0.15	10/13
IL1A	AA936768	14.8	4.58	13/13	CNK	AA489234	2.3	0.33	5/13
EGR2	AA446027	14.7	4.26	11/13	PTPN1	T57321	2.2	0.16	8/13
TNFAIP6	W93163	12.9	1.79	13/13	DDX3	AA626845	2.2	0.22	8/13
GCH1	AA443688	9.9	1.14	13/13	KIAA0680	AA700164	2.2	0.15	7/13
NFKBIA	W55872	8.7	0.93	13/13	LPL	AA633835	2.2	0.16	8/13
MAP2K6	H07920	8.7	1.57	13/13	REL	AI247359	2.2	0.19	7/13
MBL2	T69359	8.7	0.56	13/13	IER3	AA480815	2.2	0.19	6/13
LIF	R50354	8.3	1.73	12/13	CSF1	T55558	2.1	0.26	5/11
SCYA2	AA425102	7.5	2.37	5/6	AKT3	AI864214	2.1	0.31	5/12
GLS	AI004766	7.1	2.62	7/7	CTF1	AA884403	2.1	0.38	5/13
RGS16	AA453774	6.9	1.33	12/12	PIM1	AA453663	2.1	0.17	6/13
KIAA0938	AA705735	6.4	1.17	10/11	IRF1	AA478043	2.1	0.15	8/13
NFKB2	AA952897	6.1	1.17	11/13	ZNF297B	AA465708	2	0.17	6/13
DUSP2	AA759046	5.9	0.64	13/13	BCL2L2	AA456480	2	0.21	6/13
NGFB	T56316	5.7	0.88	13/13	FGF9	AA946776	2	0.14	8/13
PLAU (uPA)	AA284668	5.5	0.78	13/13	TGFBR3	H62473	2	0.16	5/12
JUNB	N94468	5.2	0.77	11/11	HIF1A	AA598526	1.9	0.12	7/13
NFE2L2	H88359	4.6	0.36	13/13	KAL1	H92621	1.9	0.19	6/12
ITGA2	AA463610	4.6	0.85	6/7	SOX9	AA400739	1.9	0.15	5/11
TWIST	AI220198	4.4	0.66	10/13	ESMI	W46577	1.7	0.15	5/12
RIPK2	AA913804	4.2	0.26	13/13	DTR	R14663	1.2	0.63	5/13
JUN	W96134	4.2	0.82	10/13	PPP1R15A	AA460168	−1.5	0.23	5/13
PTGER2	AI276745	3.8	0.81	10/13	NET1	R24543	−1.6	0.17	5/13
KIAA0298	AA853966	3.8	0.40	11/13	ICAM5	R87840	−1.7	0.15	5/13
NAB1	N91896	3.7	0.18	13/13	PM5	AA629923	−1.8	0.10	5/13
SCYB10	AA878880	3.7	0.78	8/13	GFPT1	AA478571	−1.9	0.12	5/13
PDE4B	AA453293	3.6	0.39	13/13	GCNT1	AI657057	−1.9	0.17	5/13
SLC9A6	R45009	3.5	0.34	13/13	CYP1B1	AA448157	−2	0.27	7/13
PTGER3	AA151583	3.4	0.70	7/12	PPP1R8	N99208	−2.1	0.08	7/13
UNG2	AA425900	3.4	0.34	11/13	PPAT	AA873575	−2.1	0.21	7/13
BIRC3	H48706	3.3	0.46	10/13	CXCR4	T62491	−2.1	0.21	7/13
C7	AA598478	3.1	0.28	11/13	KIAA0711	AA702544	−2.3	0.23	7/13
KIAA0105	AA598802	3.1	0.24	12/13	PCDH8	H29216	−2.3	0.20	8/13
GAD1	AA018457	3	0.35	11/13	SREBF1	AA425823	−2.4	0.29	7/13
CBLN1	AA495901	2.9	0.21	12/13	CITED2	AA115076	−2.4	0.42	6/13
SNK	AA460152	2.9	0.35	9/13	CCND3	AI340905	−2.6	0.76	5/13
C8orf1	AA278836	2.9	0.24	11/13	ITPKB	R94153	−2.8	0.29	9/12
TIEG	AI348177	2.8	0.15	12/13	CENPA	AI369629	−3.2	0.35	11/13
OLR1	AA682386	2.6	0.24	9/12	SERPINB2	T49159	−3.2	0.66	7/13
DBY	AA447588	2.6	0.14	11/13	B3GNT1	H93550	−3.5	0.56	5/6
BCL2	H74208	2.6	0.34	9/13	THBD	H59861	−3.6	0.38	12/13
CHL1	H15267	2.6	0.40	5/9	MYC	AA464600	−3.7	0.42	11/13
XBP1	W90128	2.6	0.26	9/13	GFI1	AA418008	−5	0.54	13/13

[a] GenBank accession of the clone on the array.
[b] Data were collected from 13 independent cell treatments. Genes shown changed twofold up or down in at least five treatments. Change is the average from all measurements for this gene centered around 1, meaning no change.
[c] Number of times the gene showed a twofold change/number of measurements for this gene.
[d] The IL8 probe was cloned at the Lerner Research Institute.

including those encoding AU-rich transcripts (38, 50). In order to boost the levels of AU-rich mRNAs and activate p38, THP-1 cells were treated with LPS for 2 h prior to initiating mRNA decay. As expected, the LPS treatment induced cellular differentiation from a round suspension cell to an adherent macrophage-like phenotype (1). Cell differentiation was accompanied by the transcriptional response of ARE-containing genes, which was measured by cDNA array hybridization on the AU array. Ninety genes were induced and 22 were repressed to at least twofold in LPS-treated compared to untreated cells in at least 5 of 13 independent treatments (Table 1).

The highest levels of gene induction were observed for cy-

tokines, including interleukin-1α, tumor necrosis factor alpha, interleukin-8, and many others that are part of the inflammatory response. In addition, several genes were identified that, to the best of our knowledge, have not yet been described as LPS responsive. Examples are the cleavage- and polyadenylation-specific factor 6 (also known as CF Im), a nuclear protein implicated in mRNA 3′-end processing (61), which was induced 20.7-fold. Early growth response 2 (EGR2), a zinc finger transcription factor homologous to mouse Krox-20 that is coregulated with other immediate-early genes and plays a critical role in peripheral nerve myelination (11, 31, 49, 70), was induced 14.7-fold. The regulator of G-protein signaling 16 (RGS16), a member of the RGS gene family that has been implicated in attenuation of p38 activation via G protein-linked receptors (21, 70), was induced 6.9-fold. Some novel LPS-induced genes such as the antiapoptotic genes BCL2 and BCL2-like 2 and the transcription factor nuclear factor erythroid 2-like 2 (also abbreviated Nrf2) may play a role in self-defense mechanisms that are initiated by macrophages to protect themselves from nitric oxide.

The two most highly and consistently repressed genes included growth factor-independent 1 (GFI1) and c-Myc, decreasing in expression 5- and 3.7-fold, respectively. The latter was consistently repressed in accord with its role in maintaining proliferation and preventing differentiation and apoptosis. GFI1 has recently been suggested to limit inflammatory responses by interfering with the production of cytokines such as tumor necrosis factor, interleukin-10, and interleukin-1β (32), and hence, its repression by LPS appears logical in the context of a macrophage-initiated inflammatory response. Clearly, although our data are restricted to ARE-containing genes, the analysis of the transcriptional response of THP-1 cells to LPS can improve our understanding of macrophage defense against this bacterial toxin.

Identification of new AU-rich mRNAs stabilized by p38. The stress-activated p38 MAP kinase has previously been implicated in regulating the expression levels of a few genes via ARE-mediated mRNA turnover. To examine the effect of p38 activity on the mRNA stability of several hundred AU-rich genes in parallel, LPS-stimulated THP-1 cells were treated with actinomycin D or a combination of actinomycin D and SB for 30 to 240 min. Total RNA from treated and untreated cells was extracted, labeled, and hybridized to the AU array. Three series of independent cell treatments, RNA isolations, and array hybridizations were performed. The average half-lives, without and with SB, of all AU-rich genes that were detectable at reliable levels were calculated from the decrease in the signal ratio of treated over untreated samples.

LPS treatment highly activated p38 in THP-1 cells after 2 h of exposure, and the addition of 1 or 2 μM SB with or without actinomycin D inhibited p38 to equal levels. Importantly, the addition of actinomycin D alone did not influence the p38 activity but, when combined with SB, caused nearly complete inactivation of p38 (Fig. 1). For the following decay time courses, 1 μM SB was used because the inhibitor has been shown to be largely p38 specific at this low concentration (16, 17). Minor inhibition of the c-Jun N-terminal kinase (JNK) of 10 to 15% may occur at 2 μM SB (17).

Average mRNA half-lives were calculated for 470 ARE-containing and approximately 40 housekeeping genes. The remaining 480 ARE-containing genes on the array were excluded from the analysis because their initial expression level was already below our signal intensity cutoff and consequently the decay could not be measured with any statistical certainty. We identified 45 AU-rich messages that decayed at least 1.5 times and up to 6.6 times faster in the presence of the p38 inhibitor (Fig. 2). The differences in $t_{1/2}$, without and with SB, reached statistical significance ($P < 0.05$) for 11 of the 45 genes. However, it needs to be considered that this P value is based on the standard deviation and the degrees of freedom of $t_{1/2}$ (= number of time points going into the calculation). This is important because rapidly decaying messages or genes expressed at low levels will only allow accurate calculation of $t_{1/2}$ over the first two or three time points. At later time points, the mRNA will already have decayed to background levels. For example, *COX2* (Unigene symbol PTGS2) mRNA decay was accelerated upon p38 inhibition 3.5-fold, from 77 to 22 min, as previously shown in other studies, yet the P value associated with this difference in our study was 0.116. Hence, we suggest that the stability of all transcripts presented in Fig. 2. is regulated via a p38-dependent pathway.

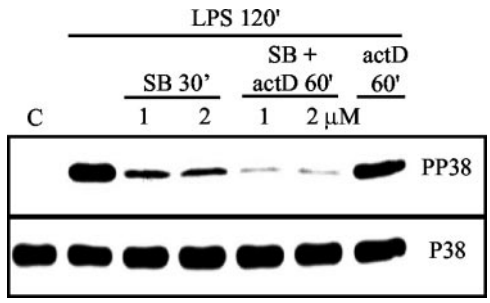

FIG. 1. Inhibition of p38 MAP kinase by SB. Shown are phospho-p38 (PP38) and total p38 (P38) Western blots of THP-1 cell extracts. Cells were not treated (C) or treated with LPS for 2 h. After 2 h of LPS incubation, treatments were either with SB alone at 1 or 2 μM for 30 min, with a combination of SB and actinomycin D (actD) for 60 min, or with actinomycin D alone for 60 min.

It should be noted that there are limitations in using actinomycin D as a tool to measure mRNA half-life, and different approaches may have to be used to arrive at consensus values. In addition to previously identified targets like *COX2*, interleukin-8, and MIP1α (SCYA3), we found 42 genes which we submit as newly identified targets for p38-mediated message stabilization. Though the majority of these were inflammatory response mediators, such as the members of the small inducible cytokine subfamilies A (SCYA2, -3, -3L1, and -4) and B (GRO-1, -2, and -3, interleukin-8, and SCYB10), and the acute-phase response mediators interleukin-1α and -1β, a variety of messages that do not appear to be directly involved in the immune response were also found to be stabilized by p38. Among these were mRNAs coding for apoptosis regulators (TNFAIP3, PMAIP6, and BCL2), transcription factors (JunB, IRF1, and SOX9), signaling kinases (MAP kinase kinase 6 and PIM1), phosphatases (PPP3CC), growth factors and receptors (FGF9 and DTR), various enzymes with metabolic, ion homeostasis, and DNA repair functions (GCH1, GAD1, CA2, PFKFB3, and UNG2), and nuclear mRNA processing factors (cleavage- and polyadenylation-specific factor 6). In summary, this variety of functionally diverse genes attests to the impor-

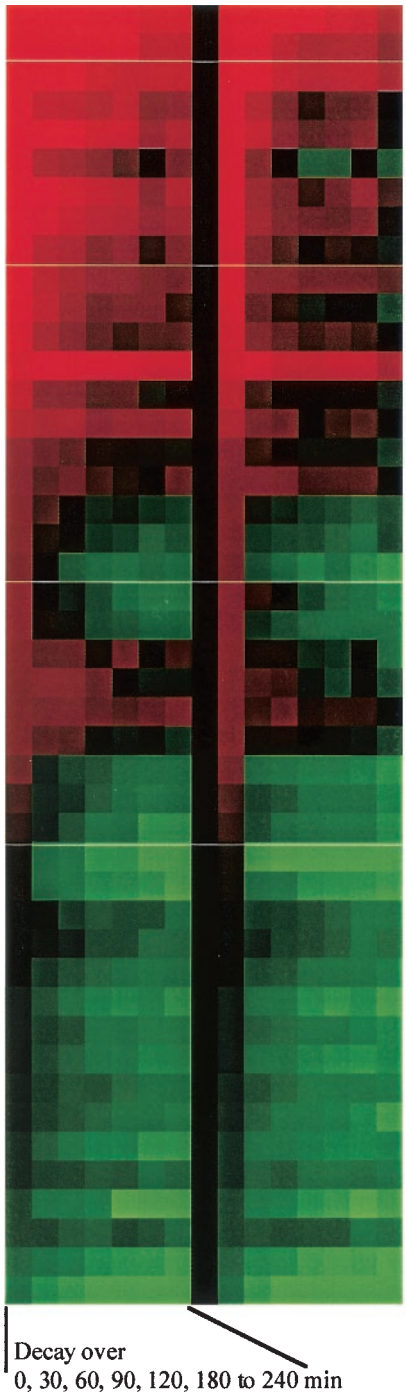

Gene	Acc	$t_{1/2}^{-SB}$	$t_{1/2}^{+SB}$	$-t_{1/2}$	*p*-value
SCYA4*	H62985	119	65	1.8	0.004
IL1B*	W47101	74	30	2.5	0.017
TNFAIP3*	AA476272	34	22	1.5	0.084
GRO1*	W42723	49	18	2.7	0.000
SCYA3L1*	R47893	56	18	3.0	0.076
GRO2*	R50407	29	13	2.2	0.000
IL8*	AA102526	45	17	2.6	0.027
CPSF6*	R18985	75	18	4.1	0.004
GRO3*	AA935273	57	29	2.0	0.007
SCYA3*	AA677522	93	31	3.0	0.029
PTGS2*(COX2)	R80217	77	22	3.5	0.116
IL1A*	AA936768	42	16	2.6	0.222
GCH1*	AA443688	732	333	2.2	0.258
MAP2K6*	H07920	69	23	2.9	0.028
SCYA2*	AA425102	136	43	3.2	0.060
UNG2*	AA425900	65	25	2.6	0.085
SCYB10*	AA878880	131	86	1.5	0.334
BCL2*	H74208	34	17	1.9	0.289
GAD1*	AA018457	28	15	1.8	0.256
JUNB*	N94468	23	13	1.7	0.382
FGF9*	AA946776	107	62	1.7	0.018
PIM1*	AA453663	65	24	2.7	0.146
DAF*	R09561	243	85	2.8	0.056
CSF1*	T55558	438	77	5.7	0.347
IRF1*	AA478043	432	66	6.6	0.345
KIAA0410	R43334	115	50	2.3	0.343
PMAIP1*	AA458838	37	20	1.9	0.438
SOX9*	AA400739	120	36	3.3	0.100
FMR1	N48355	58	37	1.6	0.311
DTR*	R14663	36	10	3.6	0.193
ZFHX1B	AA490605	31	19	1.7	0.149
ING1	N47309	87	47	1.8	0.356
PPP3CC	W17217	134	69	1.9	0.402
C1D	N22178	83	44	1.9	0.365
CA2	H23187	69	33	2.1	0.181
STK39	AI364374	96	43	2.2	0.354
PFKFB3	AI301004	80	32	2.5	0.195
HSPC177	AA864458	126	74	1.7	0.379
BCL7A	AA281583	206	58	3.6	0.051
TRIP-Br2	AA489839	65	36	1.8	0.321
PLCB2	AA464970	137	60	2.3	0.396
PLAA	AI675369	59	37	1.6	0.429
SERPINH2	R71440	627	400	1.6	0.497
PPP1R15A	AA460168	85	31	2.7	0.135
CITED2	AA115076	122	47	2.6	0.076

FIG. 2. Differential mRNA decay upon p38 inhibition detected on the AU-rich gene array. mRNA decay rates were measured from three independent experiments on THP-1 cells with the AU-rich gene array. After 2 h of LPS treatment, transcription was blocked with actinomycin D (actD) with or without addition of SB. Genes are named with the Unigene database symbol. The stars (*) next to the name indicate genes that were induced after 2 h of LPS treatment (see Table 1). GenBank accession numbers (Acc) represent the clones used on the array. Half-lives ($t_{1/2}$), in minutes, without and with SB, were calculated as described in the text. ρ $t_{1/2}$ is the half-life ratio: $t_{1/2}^{-SB}/t_{1/2}^{+SB}$ and the *P* values indicate the statistical significance of this ratio. Shown here are all genes identified in this study that decayed at least 1.5-fold faster upon p38 inhibition (ρ $t_{1/2} > 1.5$). The colored boxes (produced with TreeView by Michael Eisen, Lawrence Berkeley National Laboratory) indicate decline in mRNA levels over the decay time course from 0 to 240 min (red to green). Genes are sorted in descending order by initial expression level at 0 min. The two columns of colored boxes are separated by pale lines into five blocks. Each block has a different contrast setting, and hence the colors between blocks are not directly comparable. This was necessary to allow better horizontal comparison of the left and right column for each gene.

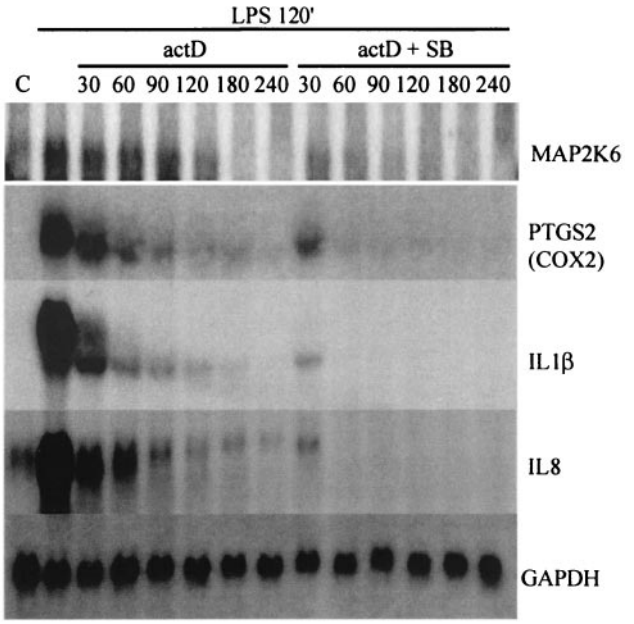

FIG. 3. Differential mRNA decay of MAP kinase kinase 6 (MAP2K6), *COX2*, interleukin-1β (IL1β), and interleukin-8 (IL8) on p38 inhibition detected by Northern blot. The samples used here are identical to one of the three used in the mRNA decay time course experiments in the array hybridizations. See the text for a description of the cell treatments. Times are in minutes. Lane C, no-treatment control. GAPDH, glyceraldehyde-3-phosphate dehydrogenase.

tance of the p38 pathway in the posttranscriptional regulation of gene expression for the class of ARE-containing genes.

To confirm the array results for different genes with an alternative method, Northern blotting analyses were performed on RNA from one of the three time courses, probing for MAP kinase kinase 6, *COX2*, interleukin-8, interleukin-1β, and glyceraldehyde-3-phosphate dehydrogenase (Fig. 3). Densitometry of the Northern blots for the last four was compared with the mRNA decay measured on the AU array. The results (Fig. 4) indicate that there is a tight correlation with the results obtained by densitometry of the Northern blots compared to array analysis for the three ARE-containing genes tested.

Stability of 425 AU-rich mRNAs in LPS-treated THP-1 cells regulated independently of p38. In addition to identifying genes that appeared to be stabilized by p38, we determined the half-lives of 425 AU-rich mRNAs that were not destabilized greater than 1.5-fold upon p38 inhibition in our study (Table 2). Other studies have reported that interleukin-3, interleukin-6, tumor necrosis factor alpha, and urokinase-type plasminogen activator are stabilized by p38 activation (4, 47, 48, 70). However, we did not detect any significant changes in the half-lives of these messages in our THP-1 cell experiments. For example, tumor necrosis factor alpha had the shortest half-live of all AU-rich mRNAs in all three repeat experiments in the presence and absence of the p38 inhibitor (averaged $t_{1/2}{}^{-SB} = 7.6$, $t_{1/2}{}^{+SB} = 6.9$ min). This discrepancy with other studies may be due to differences in the cell system, such as the use of fresh human blood monocytes, HeLa, or NIH 3T3 cells, or differences in experimental design or method of detection, and it seems likely that the list of genes presented in Table 2 may contain mRNAs that might be stabilized or destabilized by p38 activation under different conditions.

We investigated whether the number of AUUUA motifs that are present in the AREs are indicative of the half-life that one can expect for a particular message (Fig. 5). The genes in the ARED had previously been clustered on the basis of the number of ARE motifs (2). Clustering the mRNAs based on the determined half-lives into two groups, one with a $t_{1/2}$ of <100 min and the other one with a $t_{1/2}$ of >100 min (100 min was the mean of the ARE mRNA half-lives), we used analysis of variance (ANOVA) between groups to test the hypothesis that mRNAs with more AUUUA motifs are more likely to have a shorter half-life than those with fewer motifs. The resulting ANOVA P value of less than 0.0001 verified this hypothesis.

However, our analysis also showed that the presence of the AUUUA motif is not entirely predictive of a short half-life (<100 min). A recent study of mRNA turnover that used the ARE mRNA clustering provided in the our database found that AREs are present more frequently in short-lived mRNAs, yet some messages with half-lives longer than 8 h also contained the AUUUA motif (36). ARE mRNAs were also clustered into the class I and class II categories of Chen et al. (12), in which class I has discontinuous nonamers and class II has at least two overlapping copies of the nonamer. When the half-lives in each category were compared, we found that the means of half-lives in class I (121 ± 8 min) and II (84 ± 19) were marginally different but not statistically significant (Fig. 6). However, when LPS-induced ARE mRNAs were clustered, class II mRNAs had significantly ($P = 0.006$; unpaired t test with Welsh's variance correction) shorter half-lives (mean = 56 ± 6 min) compared to class I mRNAs (114 ± 19 min).

DISCUSSION

Using a computational approach, we previously identified many hundred genes, compiled in the ARE mRNA database, that have one to several copies of the AUUUA motif in the mRNA 3′ untranslated region (2). Examination of the ARE mRNA targets of the ELAV homolog protein HuB (65), which is specific to neuronal cells, showed that there were few mRNA targets in common with our array targets (notably cyclin D1, c-*myc*, and integrin B). In contrast, almost all of the previously reported mRNA targets for the ubiquitously expressed ARE-binding protein HuR, including tumor necrosis factor alpha, c-*fos*, granulocyte-macrophage colony-stimulating factor, cyclooxygenase, interleukin-3, vascular endothelial growth factor, interleukin-8, and transforming growth factor beta, are part of our array targets compiled on the basis of an ARE motif defined by bioinformatics and statistically (2).

In the present study, we used our database to make a custom cDNA array with probes representing 950 AU-rich mRNAs in order to determine the p38 dependence of mRNA stability for several hundred ARE-containing transcripts in human THP-1 monocytic cells. A role for the p38 pathway in controlling mRNA stability has so far been demonstrated for nine ARE-containing genes involved in cellular immunity, and the ARE-mediated message stabilization via p38 and the downstream MAP kinase-activated protein kinase 2 appears to be sequence specific, since the AREs of *COX2* but not of c-*myc* or tumor

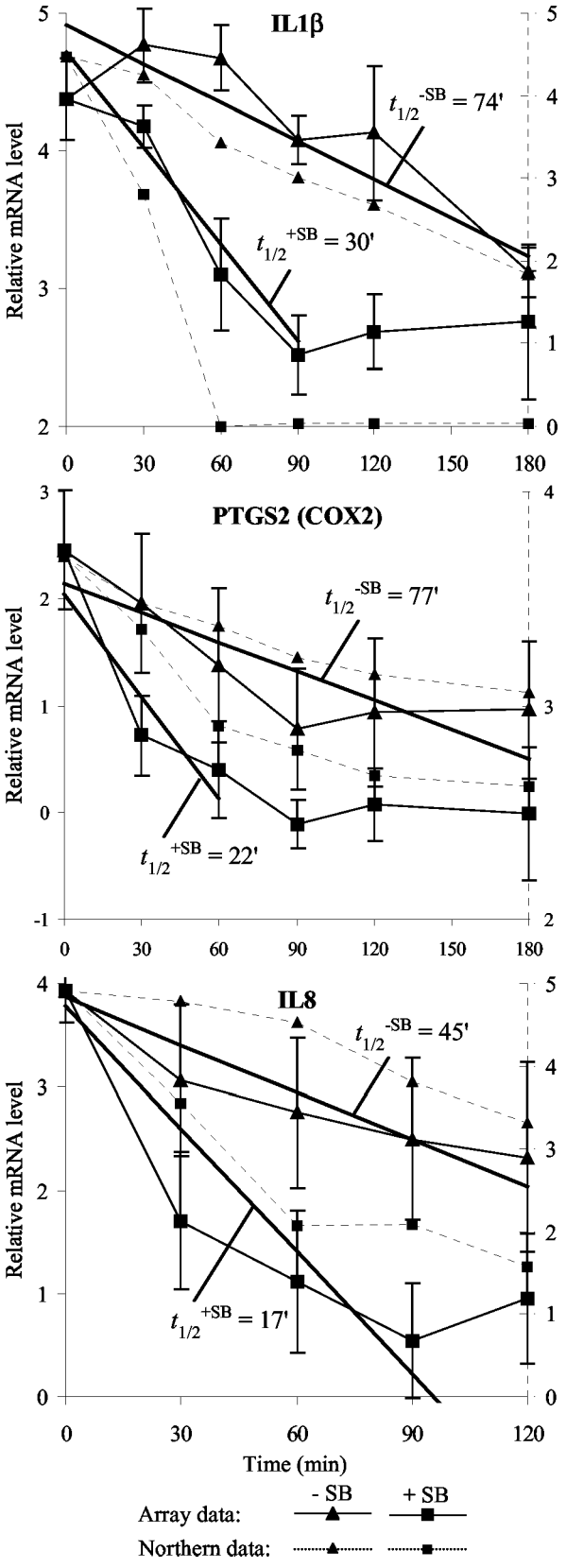

FIG. 4. p38-dependent differential mRNA decay of interleukin-1β (IL1β), *COX2*, and interleukin-8 (IL8): correlation of cDNA array and Northern blot data. Shown here are the graphs of array (solid lines) and Northern (dotted lines) data for interleukin-1β, *COX2,* and interleukin-8 mRNA decay. The array data are averages of log-transformed normalized ratios of treated over untreated samples from three repeats with standard deviations (solid *y* axis). The linear regression through the time points used in the half-life ($t_{1/2}$) calculation is shown as a bold line with the respective $t_{1/2}$ indicated (in minutes) (see text for details). The Northern data are glyceraldehyde-3-phosphate dehydrogenase-normalized, log-transformed signal intensities determined by densitometry from the Northern blots shown in Fig. 3 (dotted *y* axis).

necrosis factor alpha were able to confer p38-dependent stabilization on a β-globin reporter gene in HeLa-TO cells (39). Here we have identified 42 new candidates for message stability regulation by p38 by interrogating hundreds of AU-rich mRNAs in parallel. In addition, we have presented a transcription profile of AU-rich transcript induction and repression by LPS that is based on 13 independent cell treatments and array hybridizations, and furthermore we have submitted half-lives for 425 AU-rich mRNAs that did not show stabilization by p38 in this study.

When comparing the list of ARE-containing genes that were induced by LPS with those that we found to be destabilized upon p38 inhibition, one can make two important observations that differentiate regulation at the transcriptional and post-transcriptional levels. First, many ARE-containing genes that were induced by LPS were not stabilized at the mRNA level through the p38 pathway. This observation is not surprising because LPS signaling through Toll-like receptor 4 can activate the p38 as well as the nuclear factor-κB kinase pathways via TAK1, which can subsequently turn on different sets of target genes (13, 40, 57, 66). Second, we found a number of mRNAs that were destabilized by the p38 inhibitor but not upregulated upon LPS stimulation. This finding demonstrates for the first time that the p38 pathway can control the stability of some AU-rich mRNAs that are not transcriptionally induced upon p38 activation.

A number of genes identified in this study are of particular interest in terms of the cellular response of monocytes to LPS. Regarding the signaling through the p38 pathway, it should be noted that the MAP kinase kinase 6, one of the major upstream activators of p38 (27, 53), was strongly induced by LPS (8.7-fold) and destabilized upon p38 inhibition. This finding suggests that a positive feedback loop in the p38 pathway exists that may use transcriptional induction as well as message stabilization of MAP kinase kinase 6 in order to potentiate and/or prolong the signal.

Activated macrophages produce nitric oxide as an antimicrobial and antitumor effector molecule. Okada et al. established a link between self-defense against synthesized nitric oxide and induction of Bcl2-like 1 in LPS-treated macrophages, suggesting that upregulation of this antiapoptotic factor may contribute to macrophage survival (52). Similarly, we found that Bcl2 and Bcl2-like 2 were induced by LPS, suggesting that modulation of expression of several Bcl2 family members counteracts apoptosis to promote macrophage survival. A second line of defense employed by macrophages is the upregulation of autoprotective intracellular redox buffering systems (23, 56). A novel candidate potentially involved in this process could be the nuclear factor erythroid 2-like 2 gene,

TABLE 2. P38-independent half-lives of 425 AU-rich mRNAs[a]

Gene	ID	$t_{1/2}$	Gene	ID	$t_{1/2}$	Gene	ID	$t_{1/2}$
AB026190	AA479295	63	CRLF3	AI240562	37	HERC3	AA282253	57
ABCE1	T70122	65	CRSP2	AA150093	650	HIF1A	AA598526	80
ABR	W24076	98	CRTAP	AA486278	62	HIVEP2	AA683219	194
ACADM	N70794	108	CSF2	AA995402	39	HK1	AA485272	38
ACADSB	H96140	40	CSPG2	AA101875	193	HNRPA2B	W02101	81
ACTR1A	AI014416	273	CTF1	AA708512	39	HSPC019	AI017010	171
ADAM9	H59231	75	CUL3	H98621	72	HSU79274	AA451900	91
ADK	R12473	328	CXCR4	T62491	51	ID2	AA482267	31
AGL	AA668425	51	CYP1B1	AA448157	86	IDH3A	AA464206	71
AKT1	W77811	49	CYP51	AA477893	51	IER3	AA480815	71
ALTE	AA630498	187	DAZ	AA133797	71	IFNA1	M29884*	35
AP3M2	R14443	222	DBT	R89083	32	IFNAR1	N59150	67
APACD	AA085749	110	DBY	W37634	101	IFNB	M28622*	138
APM1	H45617	84	DDEF2	N70773	153	IGF1	N67876	47
ARCN1	AA598401	74	DDX11	AA032090	88	IL10	M57627*	155
ARFD1	AA706974	28	DDX16	AA457157	137	IL10RA	AA437226	81
ARHGEF7	AA452871	254	DDX18	R08935	76	IL12B	M65272*	93
ARHGEF9	AA147072	113	DDX3	AA626845	58	IL17	U32659*	101
ARPC5	W55964	124	DDX8	AA458473	64	IL1RAP	AA256132	134
ATP1B1	AA598814	42	DIS3	H03208	45	IL2	S77834*	38
ATP2A2	H85355	98	DLEU2	N25204	137	IL24	AA281635	247
ATP6E	AI986422	245	DMTF1	AA129860	103	IL3	M14743*	124
ATP6F	AA480826	941	DMXL1	N29992	48	IL4	M13982*	37
ATRX	AA410435	66	DSCR3	R97540	119	IL5	X12705*	89
AUH	AA448711	52	DUSP2	AA759046	17	IL6	M14584*	204
B3GNT1	H93550	29	DYRK1A	AA676749	48	IMPA1	H90219	61
B4GALT3	AA424578	63	E2F1	AA424950	88	IQGAP1	AA598496	118
BACH	AA035455	199	EDN3	T67005	90	ITGA2	AA463610	51
BCL2L2	AA456480	47	EDNRB	H28710	65	ITGAV	AA029934	251
BIRC2	R19628	101	EEF2	R20379	187	ITSN1	AA496795	181
BIRC3	AA002126	67	EGR2	AA446027	16	JUN	W96134	17
BLZF1	R43576	89	EHHADH	R02373	30	KAL1	H17882	47
BMP6	AA424833	31	EIF2AK3	AA436178	139	KDR	AA026831	57
BNIP3	AA063521	57	EIF3S1	AA455070	54	KIAA0010	AA284599	91
BPNT1	AA197334	46	EIF4E	AA193254	90	KIAA0022	H60460	64
BRCA2	H48122	55	EIF4G3	N92469	184	KIAA0028	H19822	193
BRD2	AA918860	89	ENC1	H72122	46	KIAA0040	AA465479	62
BRP441	AA459690	174	ENDOFIN	R26672	42	KIAA0141	AA455516	103
BSN	H18306	68	EPB49	N55461	31	KIAA0171	H15458	73
BTAF1	AA120777	76	ESM1	W46577	77	KIAA0212	AA630346	115
BTF	H21107	51	EVI5	T65001	53	KIAA0232	AA406589	75
BTN2A1	H68107	110	EZH2	AA430744	132	KIAA0247	N63733	81
BUB3	H38804	105	F2R	N20407	52	KIAA0254	N75979	116
BYSL	AA701929	148	F3	AI313387	56	KIAA0266	AA598993	37
C1orf16	AA431423	73	FACL4	AA633818	112	KIAA0296	AA890161	37
C1orf29	AA410567	54	FCER1G	H79353	697	KIAA0298	AA853966	20
C20orf45	AA004210	63	FKBP4	AA932521	157	KIAA0354	AA062802	62
C4orf1	AA757427	76	FUT4	R28447	67	KIAA0375	W49494	75
C7	AA598478	81	G3BP2	AA151214	177	KIAA0419	AA625653	58
C8orf1	AA027049	139	GABPB2	AW571916	224	KIAA0426	AA708279	45
CALU	R78585	231	GALC	W85914	452	KIAA0431	AA172053	44
CAP350	AI001846	41	GAS41	T62072	65	KIAA0438	AA142966	63
CASP7	T50828	274	GC20	AA488391	341	KIAA0441	N24789	27
CBLN1	AA495901	143	GCA	R44739	85	KIAA0475	AA419200	75
CBX3	AA682719	69	GCP3	AI004751	253	KIAA0476	AA282577	730
CCT2	N38959	70	GFI1	AA418008	47	KIAA0537	AA774839	110
CD164	AA598561	191	GLO1	AA136710	103	KIAA0560	AA121387	69
CD36	N39161	295	GLS	R89349	41	KIAA0628	N56973	42
CDC27	T81764	122	GMFB	H22652	190	KIAA0669	W60983	50
CDC42	AA009697	667	GNE	T68440	44	KIAA0680	AA700164	136
CDC7L1	N62245	54	GNG10	AA460286	121	KIAA0685	AA490924	272
CDK2	AI653017	424	GOT1	H22856	563	KIAA0711	AA702544	60
CDKN2D	R77517	93	GPC1	AA455896	208	KIAA0798	T90374	32
CENTB2	AA490493	104	GRB10	AA136336	67	KIAA0808	N66992	60
CHS1	N74383	70	GS2NA	AA418918	122	KIAA0844	AW131755	316
CHSY1	AA703453	61	GS3786	H88599	79	KIAA0938	AA705735	40
CIAS1	AW468866	39	GTF2A2	T55801	89	KIAA0970	R36431	47
CNK	AA489234	57	GTF2B	H23978	75	KIAA0982	AA017133	71
COX17	AA099855	76	GYS2	N72934	62	KIAA0997	R28471	38
CREBBP	AA023014	57	HCS	R52654	172	KIAA1041	AA629800	70
CREG	T71991	389	HD	T64094	83	KIAA1046	R78541	66

Continued on following page

TABLE 2—*Continued*

Gene	ID	$t_{1/2}$	Gene	ID	$t_{1/2}$	Gene	ID	$t_{1/2}$
KLHL2	AI348818	541	PLAU	AA284668	62	SRRM1	R26536	65
KMO	R44396	105	PLCL1	AI222930	37	SSFA2	AA496804	167
KNSL1	AA504625	83	PLOD2	H99816	204	ST13	H65676	170
KNTC1	AA157787	79	PM5	AA025160	895	STAU	AA669068	217
KPNA1	AA180046	175	POU6F1	N63968	71	STIM1	AA157018	287
KRAS2	AA505084	65	PPP1R8	N99208	143	STIP1	AA487635	157
LEPR	AI208285	72	PPP2CA	AA599092	79	STK17A	AA453754	78
LEPROTL1	T62031	134	PPP3CA	AA682631	52	STK3	AA136675	43
LIF	R50354	117	PPP3CB	AA015621	82	SYBL1	R27644	172
LIM	R92455	52	PRC1	AA449336	69	TACC1	AA664006	105
LIV-1	H29407	127	PREI3	AA410302	53	TAF7	AA461518	79
LMAN1	AA446103	112	PREP	AA664056	93	TBCC	AA954188	43
LOC51026	R69622	87	PRG4	AA280514	127	TBP	N50549	146
LOC51071	N74602	80	PRKX	AA778448	38	TBX2	N99243	209
LPL	AA633835	175	PSMD10	R77104	256	TCF12	AA488497	54
LRP8	AA527256	168	PSMD12	AA497132	85	TCFL4	AA134555	66
LTA	W72329	66	PTBP1	AA677517	156	TDE1	AA679489	221
M6PR	AA465223	189	PTK2B	R85257	331	TDG	T91074	62
MADD	AA282445	154	PTPN1	T57321	365	TEB4	H67086	64
MAN1	AA520992	67	PTPRA	H82419	79	TG737	AA481585	63
MATN3	AI375563	41	PTPRC	H74265	249	THBD	H59861	53
MBL2	T69359	17	PWP2H	H50886	299	THBS1	AA464630	54
MBTPS1	AA447393	112	RABIF	AA012984	53	TIEG	AI348177	18
MEF2C	AA234897	60	RAD21	AA683102	84	TIMM17A	AA708446	69
METAP2	AA283030	180	RB1	AA045192	87	TMEM1	N94245	122
MICB	H69835	59	RB1CC1	AA047435	59	TNF	AA699697	8
MLLT2	AA057425	53	RBBP8	H23021	96	TNFAIP6	W93163	145
MMD	AA487643	147	RBL2	N50554	79	TNFSF9	AA778663	36
MMP1	AA143201	112	RCN2	AA598676	81	TOMM20	AA644550	74
MNAT1	AA481759	247	REL	AI247359	111	TOPBP1	R97785	48
MPP2	H39068	68	RGS16	AA453774	14	TPD52	AA459318	123
MRPL33	AA489478	81	RI58	W24246	71	TPP2	T77959	63
MTHFD2	AI361330	192	RIPK2	AA913804	72	TRAF4	AA598826	239
MTM1	AA491225	128	RMS1	R77718	42	TRAF5	AA102634	53
MTMR2	AA436164	94	RNF11	W94868	80	TRAP240	AA434084	105
MTR	AA233650	64	RNF14	N62157	70	TRPM1	N35472	40
MYC	AA464600	32	RNGTT	AW137353	57	TSNAX	AA477514	133
MYO1E	AA029956	49	ROR2	AA149251	96	TWIST	AI220198	30
NAB1	N91896	118	RTVP1	AA251800	91	TXNRD1	AA453335	113
NCAM2	AA709271	95	RYK	T77810	84	UAP1	N68465	116
NEK4	AA496013	44	SAC2	R69354	43	UBA2	H11320	69
NEURL	N30706	55	SBB103	AI299601	166	UBE2A	AA600173	204
NFE2L2	AA629687	51	SC5DL	AA216535	63	UBE2H	AA520978	150
NFKBIA	W55872	23	SCAP2	R81177	49	UBE2V2	AA448676	80
NGFB	T56316	46	SCYA11	W69211	53	UBL3	AA151852	126
NICE-3	N76101	138	SCYA16	T58775	59	UGCG	N90204	125
NMT2	AA664135	33	SCYD1	R66139	75	UGDH	AA992570	59
NOVA1	AI362062	144	SDFR1	AA130671	187	UK114	AI301696	207
NR3C1	AA664219	93	SEMA3B	AA455145	82	USP6	AI203661	40
NR4A1	N94487	278	SEP15	AA999842	191	USP8	AI299198	59
NR4A3	H37761	99	SERPINB2	T49159	33	VBP1	AA478108	162
NR6A1	AA853954	226	SFRS11	AA481054	239	VEGF	R19956	106
OGDH	AA856769	744	SHOX2	AA425419	81	VPS26	AA064946	108
ORC6L	N90667	57	SIP	W87541	121	VPS41	AA143559	137
OSR1	R98985	213	SIRPB1	AI088704	38	WBP4	AA702632	69
P115	AA504342	79	SIRT1	AA460952	41	WDR3	AA775806	97
PAIP1	AA598533	104	SLC26A4	AI139968	32	WHSC1	AA159311	121
PARG1	AA629603	26	SLC2A1	R17667	42	WRB	AA099383	93
PCDHA9	AA437139	56	SLC2A3	H52531	33	WS-3	AA451781	415
PCK1	AA405769	47	SLC35A2	H51549	370	WSB1	AA025807	64
PDE4B	AA453293	23	SLC9A6	R45009	45	WTAP	AA598802	200
PDE7A	AA992565	48	SLK	W17289	143	XBP1	W90128	52
PDGFB	W68169	70	SMN1	AA004858	64	XPR1	AA453474	123
PDX1	N48320	125	SNAP25	AA663884	456	YES1	H56929	49
PER1	T95053	34	SNAPC3	AA043334	268	ZFX	AI740859	97
PEX1	AA598527	148	SNK	AA460152	23	ZMPSTE24	AA001403	115
PGK1	AA599187	163	SPG4	AA171421	61	ZNF198	AA251581	114
PIGN	AA033974	138	SPTBN1	H98241	117	ZNF207	N59119	71
PIK3CD	AA281784	100	SRF	AA487973	152	ZNF238	R79722	79
PKD1	N27758	56	SRPK1	AA630604	140	ZNF297B	AA702698	47
PLAT	R38933	163	SRPR	AA598621	327			

[a] Genes are named with the Unigene Database symbol and ordered alphabetically. IDs are GenBank accession numbers of the clone on the array. *, probes generated by reverse transcription-PCR. $t_{1/2}$ (in minutes) was determined without p38 inhibition; calculation from three independent experiments as described in the text.

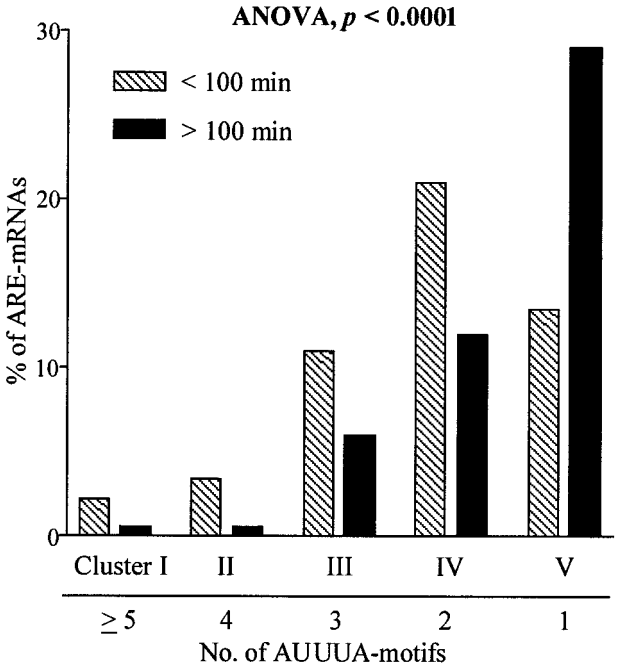

FIG. 5. ARE mRNA half-lives correlate with the number of AUUUA motifs. ARE-containing mRNAs were clustered into five groups according to the number of AUUUA motifs in the 3′ untranslated regions, and their respective half-lives were clustered in two groups (<100 min and >100 min). Analysis of variance between groups (ANOVA) shows that the number of AUUUA motifs is indicative of half-life.

which was induced by LPS 4.6-fold. This basic leucine zipper transcription factor has been implicated in the regulation of expression of detoxifying genes (10, 29) and, when deficient in mice, causes increased susceptibility to oxidative stress (9).

A gene that was stabilized through p38 but not transcriptionally induced by LPS was carbonic anhydrase 2. Carbonic anhydrases are of great physiological importance in many biological processes, including respiration, calcification, acid-base balance, bone resorption, and others (20). As catalysts of the reversible hydration of carbon dioxide, they are critical in maintaining the cellular CO_2/HCO_3^- buffering system. Recent findings suggested that carbonic anhydrase may be important in inflammatory processes, because ambient pCO_2 can modulate neutrophil activity by altering intracellular pH, thereby affecting intracellular oxidant generation and interleukin-8 secretion after LPS stimulation (14). Therefore, carbonic anhydrase 2 may also play a role in maintaining intracellular pH levels in activated macrophages, and hence, it would appear logical to stabilize the carbonic anhydrase 2 mRNA in a p38-dependent manner.

The macrophage-specific colony-stimulating factor 1 was also among the p38-stabilized messages. This regulation is noteworthy because macrophage-specific colony-stimulating factor 1 may regulate host responses to pathogens by modulating Toll-like receptor expression as treatment of macrophages with macrophage-specific colony-stimulating factor 1 downregulated Toll-like receptor 1, 2, 6, and 9 expression but not the LPS receptors Toll-like receptor 4 and 5 (64).

From an evolutionary viewpoint, we find it intriguing that the five CXC chemokines interleukin-8, GRO1, GRO2, GRO3, and SCYB10, which all showed p38-dependent message stability in our study, belong to a multigene family on

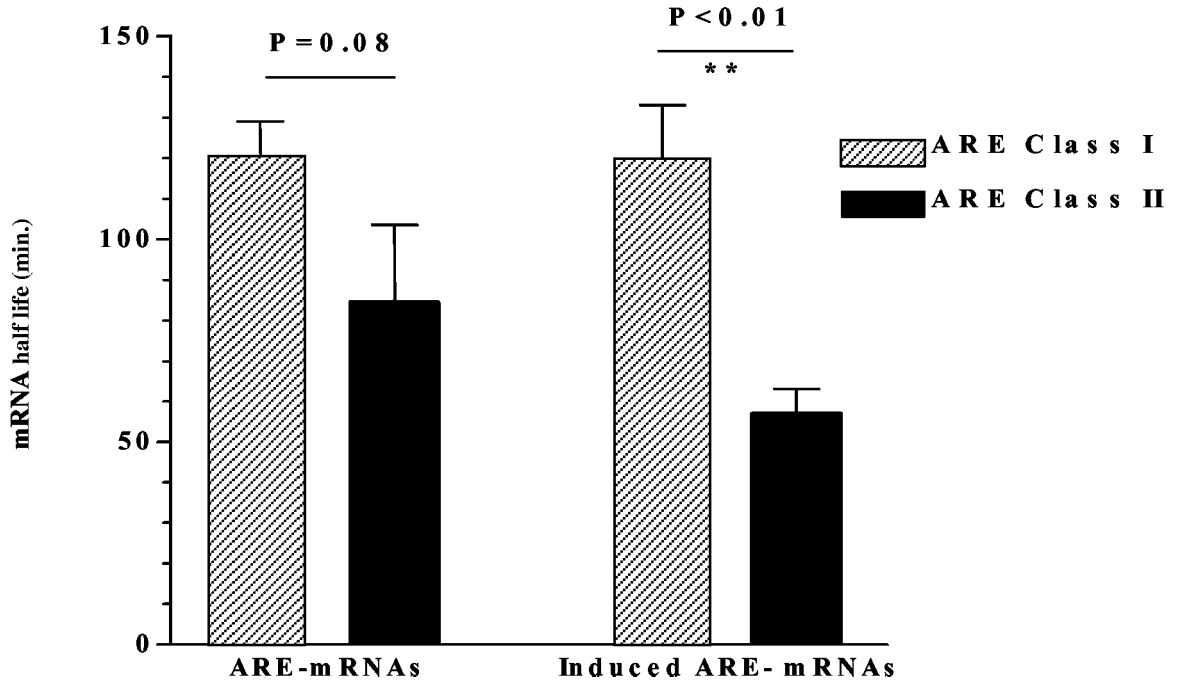

FIG. 6. Class II LPS-induced ARE mRNAs have shorter half-lives than class I. ARE mRNAs were clustered into two categories, class I and class II, which have either discontinuous nonamers or at least two overlapping copies of the nonamer, respectively (12). Subsequently, the half-lives in each category were compared.

chromosome 4 that most likely arose by gene duplication (51). This correlation may indicate that controlling mRNA stability could be an ancestral mechanism that developed early in the evolution of immune response regulation.

When considering the practical application of this study, it should be noted that ARE-containing genes identified as posttranscriptionally regulated by p38 are involved in different diseases. For example, interleukin-1 is expressed at abnormally high levels by glial cells in Alzheimer's disease, possibly contributing to the pathophysiology of the disease (60). Interleukin-1 was also implicated in cases of rheumatoid arthritis with severe erosive disease (15) and in early-onset periodontitis (19). For ARE mRNAs implicated in disease, the knowledge of this regulation may warrant consideration of drug intervention that may influence gene expression at the level of mRNA stability. However, the degree to which the posttranscriptional regulation of the 42 novel p38 target genes contributes to their overall level of expression and the physiological importance of this regulation will first need to be assessed on a gene-by-gene basis in the appropriate cell systems.

In conclusion, this study has provided new insights into the regulatory networks that control the response of monocytes to LPS and underlined the importance of the posttranscriptional regulation of AU-rich mRNAs through the p38 MAP kinase signaling pathway. The identification of the 42 new AU-rich transcripts that are regulated via p38 at the level of mRNA stability will further aid in understanding the molecular mechanisms by which this regulation occurs.

ACKNOWLEDGMENTS

This work was supported in part by National Institutes of Health grants RO1-AI34039 and PO1-CA62220.

REFERENCES

1. **Adams, D. O., and T. A. Hamilton.** 1984. The cell biology of macrophage activation. Annu. Rev. Immunol. **2:**283–318.
2. **Bakheet, T., M. Frevel, B. R. Williams, W. Greer, and K. S. Khabar.** 2001. ARED: human AU-rich element-containing mRNA database reveals an unexpectedly diverse functional repertoire of encoded proteins. Nucleic Acids Res. **29:**246–254.
3. **Bevington, P. R., and D. K. Robinson.** 1992. Method of least squares, p. 53–62. *In* P. R. Bevington and D. K. Robinson (ed.), Data reduction and error analysis for the physical sciences. WCB McGraw-Hill, Boston, Mass.
4. **Brook, M., G. Sully, A. R. Clark, and J. Saklatvala.** 2000. Regulation of tumour necrosis factor alpha mRNA stability by the mitogen-activated protein kinase p38 signalling cascade. FEBS Lett. **483:**57–61.
5. **Buzby, J. S., G. Brewer, and D. J. Nugent.** 1999. Developmental regulation of RNA transcript destabilization by A + U-rich elements is AUF1-dependent. J. Biol. Chem. **274:**33973–33978.
6. **Carballo, E., H. Cao, W. S. Lai, E. A. Kennington, D. Campbell, and P. J. Blackshear.** 2001. Decreased sensitivity of tristetraprolin-deficient cells to p38 inhibitors suggests the involvement of tristetraprolin in the p38 signaling pathway. J. Biol. Chem. **276:**42580–42587.
7. **Carballo, E., W. S. Lai, and P. J. Blackshear.** 1998. Feedback inhibition of macrophage tumor necrosis factor-alpha production by tristetraprolin. Science **281:**1001–1005.
8. **Carballo, E., W. S. Lai, and P. J. Blackshear.** 2000. Evidence that tristetraprolin is a physiological regulator of granulocyte-macrophage colony-stimulating factor messenger RNA deadenylation and stability. Blood **95:**1891–1899.
9. **Chan, K., X. D. Han, and Y. W. Kan.** 2001. An important function of Nrf2 in combating oxidative stress: detoxification of acetaminophen. Proc. Natl. Acad. Sci. USA **98:**4611–4616.
10. **Chan, K., and Y. W. Kan.** 1999. Nrf2 is essential for protection against acute pulmonary injury in mice. Proc. Natl. Acad. Sci. USA **96:**12731–12736.
11. **Chavrier, P., U. Janssen-Timmen, M. G. Mattei, M. Zerial, R. Bravo, and P. Charnay.** 1989. Structure, chromosome location, and expression of the mouse zinc finger gene *Krox-20*: multiple gene products and coregulation with the proto-oncogene c-*fos*. Mol. Cell. Biol. **9:**787–797.
12. **Chen, C. Y., and A. B. Shyu.** 1995. AU-rich elements: characterization and importance in mRNA degradation. Trends Biochem. Sci. **20:**465–470.
13. **Chow, J. C., D. W. Young, D. T. Golenbock, W. J. Christ, and F. Gusovsky.** 1999. Toll-like receptor-4 mediates lipopolysaccharide-induced signal transduction. J. Biol. Chem. **274:**10689–10692.
14. **Coakley, R. J., C. Taggart, C. Greene, N. G. McElvaney, and S. J. O'Neill.** 2002. Ambient pCO_2 modulates intracellular pH, intracellular oxidant generation, and interleukin-8 secretion in human neutrophils. J. Leukoc. Biol. **71:**603–610.
15. **Cox, A., N. J. Camp, C. Cannings, F. S. di Giovine, M. Dale, J. Worthington, S. John, W. E. Ollier, A. J. Silman, and G. W. Duff.** 1999. Combined sib-TDT and TDT provide evidence for linkage of the interleukin-1 gene cluster to erosive rheumatoid arthritis. Hum. Mol. Genet. **8:**1707–1713.
16. **Cuenda, A., J. Rouse, Y. N. Doza, R. Meier, P. Cohen, T. F. Gallagher, P. R. Young, and J. C. Lee.** 1995. SB 203580 is a specific inhibitor of a MAP kinase homologue which is stimulated by cellular stresses and interleukin-1. FEBS Lett. **364:**229–233.
17. **Dean, J. L., M. Brook, A. R. Clark, and J. Saklatvala.** 1999. p38 mitogen-activated protein kinase regulates cyclooxygenase-2 mRNA stability and transcription in lipopolysaccharide-treated human monocytes. J. Biol. Chem. **274:**264–269.
18. **DeMaria, C. T., and G. Brewer.** 1996. AUF1 binding affinity to A+U-rich elements correlates with rapid mRNA degradation. J. Biol. Chem. **271:**12179–12184.
19. **Diehl, S. R., Y. Wang, C. N. Brooks, J. A. Burmeister, J. V. Califano, S. Wang, and H. A. Schenkein.** 1999. Linkage disequilibrium of interleukin-1 genetic polymorphisms with early-onset periodontitis. J. Periodontol. **70:**418–430.
20. **Dodgson, S. J.** 1991. Why are there carbonic anhydrases in the liver? Biochem. Cell Biol. **69:**761–763.
21. **Druey, K. M., K. J. Blumer, V. H. Kang, and J. H. Kehrl.** 1996. Inhibition of G-protein-mediated MAP kinase activation by a new mammalian gene family. Nature **379:**742–746.
22. **Fan, X. C., and J. A. Steitz.** 1998. Overexpression of HuR, a nuclear-cytoplasmic shuttling protein, increases the in vivo stability of ARE-containing mRNAs. EMBO J. **17:**3448–3460.
23. **Ferret, P. J., E. Soum, O. Negre, E. E. Wollman, and D. Fradelizi.** 2000. Protective effect of thioredoxin upon nitric oxide-mediated cell injury in THP1 monocytic human cells. Biochem. J. **346:**759–765.
24. **Ford, L. P., J. Watson, J. D. Keene, and J. Wilusz.** 1999. ELAV proteins stabilize deadenylated intermediates in a novel in vitro mRNA deadenylation/degradation system. Genes Dev. **13:**188–201.
25. **Gao, F. B., C. C. Carson, T. Levine, and J. D. Keene.** 1994. Selection of a subset of mRNAs from combinatorial 3′ untranslated region libraries with neuronal RNA-binding protein Hel-N1. Proc. Natl. Acad. Sci. USA **91:**11207–11211.
26. **Gouble, A., S. Grazide, F. Meggetto, P. Mercier, G. Delsol, and D. Morello.** 2002. A new player in oncogenesis: AUF1/hnRNPD overexpression leads to tumorigenesis in transgenic mice. Cancer Res. **62:**1489–1495.
27. **Han, J., J. D. Lee, Y. Jiang, Z. Li, L. Feng, and R. J. Ulevitch.** 1996. Characterization of the structure and function of a novel MAP kinase kinase (MKK6). J. Biol. Chem. **271:**2886–2891.
28. **Holtmann, H., R. Winzen, P. Holland, S. Eickemeier, E. Hoffmann, D. Wallach, N. L. Malinin, J. A. Cooper, K. Resch, and M. Kracht.** 1999. Induction of interleukin-8 synthesis integrates effects on transcription and mRNA degradation from at least three different cytokine- or stress-activated signal transduction pathways. Mol. Cell. Biol. **19:**6742–6753.
29. **Itoh, K., T. Chiba, S. Takahashi, T. Ishii, K. Igarashi, Y. Katoh, T. Oyake, N. Hayashi, K. Satoh, I. Hatayama, M. Yamamoto, and Y. Nabeshima.** 1997. An Nrf2/small Maf heterodimer mediates the induction of phase II detoxifying enzyme genes through antioxidant response elements. Biochem. Biophys. Res. Commun. **236:**313–322.
30. **Jain, R. G., L. G. Andrews, K. M. McGowan, P. H. Pekala, and J. D. Keene.** 1997. Ectopic expression of Hel-N1, an RNA-binding protein, increases glucose transporter (GLUT1) expression in 3T3-L1 adipocytes. Mol. Cell. Biol. **17:**954–962.
31. **Joseph, L. J., M. M. Le Beau, G. A. Jamieson, Jr., S. Acharya, T. B. Shows, J. D. Rowley, and V. P. Sukhatme.** 1988. Molecular cloning, sequencing, and mapping of EGR2, a human early growth response gene encoding a protein with "zinc-binding finger" structure. Proc. Natl. Acad. Sci. USA **85:**7164–7168.
32. **Karsunky, H., H. Zeng, T. Schmidt, B. Zevnik, R. Kluge, K. W. Schmid, U. Duhrsen, and T. Moroy.** 2002. Inflammatory reactions and severe neutropenia in mice lacking the transcriptional repressor Gfi1. Nat. Genet. **30:**295–300.
33. **Keene, J. D.** 1999. Why is Hu where? Shuttling of early-response-gene messenger RNA subsets. Proc. Natl. Acad. Sci. USA **96:**5–7.
34. **Keene, J. D.** 2001. Ribonucleoprotein infrastructure regulating the flow of genetic information between the genome and the proteome. Proc. Natl. Acad. Sci. USA **98:**7018–7024.
35. **Lai, W. S., E. Carballo, J. R. Strum, E. A. Kennington, R. S. Phillips, and P. J. Blackshear.** 1999. Evidence that tristetraprolin binds to AU-rich ele-

ments and promotes the deadenylation and destabilization of tumor necrosis factor alpha mRNA. Mol. Cell. Biol. **19:**4311–4323.
36. **Lam, L. T., O. K. Pickeral, A. C. Peng, A. Rosenwald, E. M. Hurt, J. M. Giltnane, L. M. Averett, H. Zhao, R. E. Davis, M. Sathyamoorthy, L. M. Wahl, E. D. Harris, J. A. Mikovits, A. P. Monks, M. G. Hollingshead, E. A. Sausville, and L. M. Staudt.** 2001. Genomic-scale measurement of mRNA turnover and the mechanisms of action of the anti-cancer drug flavopiridol. Genome Biol. **2:**0041.1–0041.11.
37. **Lapucci, A., M. Donnini, L. Papucci, E. Witort, A. Tempestini, A. Bevilacqua, A. Nicolin, G. Brewer, N. Schiavone, and S. Capaccioli.** 2002. AUF1 Is a bcl-2 A + U-rich element-binding protein involved in bcl-2 mRNA destabilization during apoptosis. J. Biol. Chem. **277:**16139–16146.
38. **LaRue, K. E., and C. E. McCall.** 1994. A labile transcriptional repressor modulates endotoxin tolerance. J. Exp. Med. **180:**2269–2275.
39. **Lasa, M., K. R. Mahtani, A. Finch, G. Brewer, J. Saklatvala, and A. R. Clark.** 2000. Regulation of cyclooxygenase 2 mRNA stability by the mitogen-activated protein kinase p38 signaling cascade. Mol. Cell. Biol. **20:**4265–4274.
40. **Lee, J., L. Mira-Arbibe, and R. J. Ulevitch.** 2000. TAK1 regulates multiple protein kinase cascades activated by bacterial lipopolysaccharide. J. Leukoc. Biol. **68:**909–915.
41. **Levine, T. D., F. Gao, P. H. King, L. G. Andrews, and J. D. Keene.** 1993. Hel-N1: an autoimmune RNA-binding protein with specificity for 3′ uridylate-rich untranslated regions of growth factor mRNAs. Mol. Cell. Biol. **13:**3494–3504.
42. **Levy, N. S., S. Chung, H. Furneaux, and A. P. Levy.** 1998. Hypoxic stabilization of vascular endothelial growth factor mRNA by the RNA-binding protein HuR. J. Biol. Chem. **273:**6417–6423.
43. **Loflin, P., C. Y. Chen, and A. B. Shyu.** 1999. Unraveling a cytoplasmic role for hnRNP D in the in vivo mRNA destabilization directed by the AU-rich element. Genes Dev. **13:**1884–1897.
44. **Ma, W. J., S. Cheng, C. Campbell, A. Wright, and H. Furneaux.** 1996. Cloning and characterization of HuR, a ubiquitously expressed Elav-like protein. J. Biol. Chem. **271:**8144–8151.
45. **Mahtani, K. R., M. Brook, J. L. Dean, G. Sully, J. Saklatvala, and A. R. Clark.** 2001. Mitogen-activated protein kinase p38 controls the expression and posttranslational modification of tristetraprolin, a regulator of tumor necrosis factor alpha mRNA stability. Mol. Cell. Biol. **21:**6461–6469.
46. **Maurer, F., M. Tierney, and R. L. Medcalf.** 1999. An AU-rich sequence in the 3′-untranslated region of plasminogen activator inhibitor type 2 (PAI-2) mRNA promotes PAI-2 mRNA decay and provides a binding site for nuclear HuR. Nucleic Acids Res. **27:**1664–1673.
47. **Ming, X. F., G. Stoecklin, M. Lu, R. Looser, and C. Moroni.** 2001. Parallel and independent regulation of interleukin-3 mRNA turnover by phosphatidylinositol 3-kinase and p38 mitogen-activated protein kinase. Mol. Cell. Biol. **21:**5778–5789.
48. **Montero, L., and Y. Nagamine.** 1999. Regulation by p38 mitogen-activated protein kinase of adenylate- and uridylate-rich element-mediated urokinase-type plasminogen activator (urokinase-type plasminogen activator) messenger RNA stability and urokinase-type plasminogen activator-dependent in vitro cell invasion. Cancer Res. **59:**5286–5293.
49. **Nagarajan, R., J. Svaren, N. Le, T. Araki, M. Watson, and J. Milbrandt.** 2001. EGR2 mutations in inherited neuropathies dominant-negatively inhibit myelin gene expression. Neuron **30:**355–368.
50. **Nau, G. J., J. F. Richmond, A. Schlesinger, E. G. Jennings, E. S. Lander, and R. A. Young.** 2002. Human macrophage activation programs induced by bacterial pathogens. Proc. Natl. Acad. Sci. USA **99:**1503–1508.
51. **O'Donovan, N., M. Galvin, and J. G. Morgan.** 1999. Physical mapping of the CXC chemokine locus on human chromosome 4. Cytogenet. Cell Genet. **84:**39–42.
52. **Okada, S., H. Zhang, M. Hatano, and T. Tokuhisa.** 1998. A physiologic role of Bcl-xL induced in activated macrophages. J. Immunol. **160:**2590–2596.
53. **Ono, K., and J. Han.** 2000. The p38 signal transduction pathway: activation and function. Cell Signal. **12:**1–13.
54. **Pages, G., E. Berra, J. Milanini, A. P. Levy, and J. Pouyssegur.** 2000. Stress-activated protein kinases (JNK and p38/HOG) are essential for vascular endothelial growth factor mRNA stability. J. Biol. Chem. **275:**26484–26491.
55. **Peng, S. S., C. Y. Chen, N. Xu, and A. B. Shyu.** 1998. RNA stabilization by the AU-rich element binding protein, HuR, an ELAV protein. EMBO J. **17:**3461–3470.
56. **Pierre-Jacques, P., S. Emmanuelle, N. Olivier, and D. Fradelizi.** 2002. Autoprotective redox buffering systems in stimulated macrophages. BMC Immunol. **3:**3.
57. **Poltorak, A., X. He, I. Smirnova, M. Y. Liu, C. V. Huffel, X. Du, D. Birdwell, E. Alejos, M. Silva, C. Galanos, M. Freudenberg, P. Ricciardi-Castagnoli, B. Layton, and B. Beutler.** 1998. Defective LPS signaling in C3H/HeJ and C57BL/10ScCr mice: mutations in Tlr4 gene. Science **282:**2085–2088.
58. **Press, W. H., B. P. Flannery, S. A. Teukolsky, and W. T. Vetterling.** 1986. Do two distributions have the same means or variances, p. 464–469. *In* W. H. Press, B. P. Flannery, S. A. Teukolsky, and W. T. Vetterling (ed.), Numerical recipes. Cambridge University Press, New York, N.Y.
59. **Rodriguez-Pascual, F., M. Hausding, I. Ihrig-Biedert, H. Furneaux, A. P. Levy, U. Forstermann, and H. Kleinert.** 2000. Complex contribution of the 3′ untranslated region to the expressional regulation of the human inducible nitric-oxide synthase gene. Involvement of the RNA-binding protein HuR. J. Biol. Chem. **275:**26040–26049.
60. **Rogers, J.** 2000. An interleukin-1 alpha susceptibility polymorphism in Alzheimer's disease: new fuel for the inflammation hypothesis. Neurology **55:** 464–465.
61. **Ruegsegger, U., D. Blank, and W. Keller.** 1998. Human pre-mRNA cleavage factor Im is related to spliceosomal SR proteins and can be reconstituted in vitro from recombinant subunits. Mol. Cell **1:**243–253.
62. **Stoecklin, G., X. F. Ming, R. Looser, and C. Moroni.** 2000. Somatic mRNA turnover mutants implicate tristetraprolin in the interleukin-3 mRNA degradation pathway. Mol. Cell. Biol. **20:**3753–3763.
63. **Stoecklin, G., P. Stoeckle, M. Lu, O. Muehlemann, and C. Moroni.** 2001. Cellular mutants define a common mRNA degradation pathway targeting cytokine AU-rich elements. RNA **7:**1578–1588.
64. **Sweet, M. J., C. C. Campbell, D. P. Sester, D. Xu, R. C. McDonald, K. J. Stacey, D. A. Hume, and F. Y. Liew.** 2002. Colony-stimulating factor-1 suppresses responses to CpG DNA and expression of toll-like receptor 9 but enhances responses to lipopolysaccharide in murine macrophages. J. Immunol. **168:**392–399.
65. **Tenenbaum, S. A., C. C Carson, P. J. Lager, and J. D. Keene.** 2000. Identifying mRNA subsets in messenger ribonucleoprotein complexes by with cDNA arrays. Proc. Natl. Acad. Sci. USA **97:**14085–14090.
66. **Wang, C., L. Deng, M. Hong, G. R. Akkaraju, J. Inoue, and Z. J. Chen.** 2001. TAK1 is a ubiquitin-dependent kinase of MKK and IKK. Nature **412:**346–351.
67. **Wang, S. W., J. Pawlowski, S. T. Wathen, S. D. Kinney, H. S. Lichenstein, and C. L. Manthey.** 1999. Cytokine mRNA decay is accelerated by an inhibitor of p38-mitogen-activated protein kinase. Inflamm. Res. **48:**533–538.
68. **Warner, L. E., P. Mancias, I. J. Butler, C. M. McDonald, L. Keppen, K. G. Koob, and J. R. Lupski.** 1998. Mutations in the early growth response 2 (EGR2) gene are associated with hereditary myelinopathies. Nat. Genet. **18:**382–384.
69. **Winzen, R., M. Kracht, B. Ritter, A. Wilhelm, C. Y. Chen, A. B. Shyu, M. Muller, M. Gaestel, K. Resch, and H. Holtmann.** 1999. The p38 MAP kinase pathway signals for cytokine-induced mRNA stabilization via MAP kinase-activated protein kinase 2 and an AU-rich region-targeted mechanism. EMBO J. **18:**4969–4980.
70. **Zhang, W., B. J. Wagner, K. Ehrenman, A. W. Schaefer, C. T. DeMaria, D. Crater, K. DeHaven, L. Long, and G. Brewer.** 1993. Purification, characterization, and cDNA cloning of an AU-rich element RNA-binding protein, AUF1. Mol. Cell. Biol. **13:**7652–7665.
71. **Zhang, Y., S. Y. Neo, J. Han, L. P. Yaw, and S. C. Lin.** 1999. RGS16 attenuates gαq-dependent p38 mitogen-activated protein kinase activation by platelet-activating factor. J. Biol. Chem. **274:**2851–2857.